Inorganic Chemistry

ARTICLE

pubs.acs.org/IC

Two Novel Cyanide-Bridged Bimetallic Magnetic Chains Derived from Manganese(III) Schiff Bases and Hexacyanochromate(III) Building Blocks

Chun Yang,[†,§] Qing-Lun Wang,[*,†] Jing Qi,[†] Yue Ma,[*,‡] Shi-Ping Yan,[†] Guang-Ming Yang,[†] Peng Cheng,[†] and Dai-Zheng Liao[†]

[†]Department of Chemistry and [‡]Key Laboratory of Advanced Energy Materials Chemistry (Ministry of Education), Nankai University, Tianjin, 300071, P.R. China

[§]School of Chemical Engineering and Technology, Hebei University of Technology, Tianjin, 300130, P.R. China

Supporting Information

ABSTRACT: Two novel complexes, $[\{Mn(salen)\}_2\{Mn(salen)(CH_3OH)\}\{Cr(CN)_6\}]_n \cdot 2nCH_3CN \cdot nCH_3OH$ (**1**) and $[Mn(5\text{-}Clsalmen)(CH_3OH)(H_2O)]_{2n}[\{Mn(5\text{-}Clsalmen)(\mu\text{-}CN)\}Cr(CN)_5]_n \cdot 5.5nH_2O$ (**2**) ($salen^{2-}$ = *N*,*N*′-ethylene-bis(salicylideneiminato) dianion; $5\text{-}Clsalmen^{2-}$ = *N*,*N*′-(1-methylethylene)-bis(5-chlorosalicylideneiminato) dianion), were synthesized and structurally characterized by X-ray single-crystal diffraction. The structural analyses show that complex **1** consists of one-dimensional (1D) alternating chains formed by the $[\{Cr(CN)_6\}\{Mn(salen)\}_4\{Mn(salen)(CH_3OH)\}_2]^{3+}$ heptanuclear cations and $[Cr(CN)_6]^{3-}$ anions. While in complex **2**, the hexacyanochromate(III) anion acts as a bis-monodentate ligand through two *trans*-cyano groups to bridge two $[Mn(5\text{-}Clsalmen)]^+$ cations to form a straight chain. The magnetic analysis indicates that complex **1** shows three-dimensional (3D) antiferromagnetic ordering with the Néel temperature of 5.0 K, and it is a metamagnet displaying antiferromagnetic to ferromagnetic transition at a critical field of about 2.6 kOe at 2 K. Complex **2** behaves as a molecular magnet with *Tc* = 3.0 K.

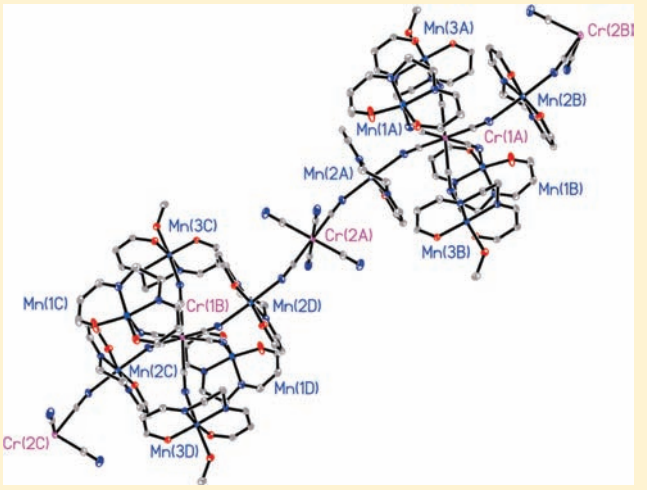

INTRODUCTION

Magnetic chain compounds have attracted continuous interest because they provide genuine opportunities to explore the fundamental aspects of magnetic interactions and magneto-structural correlations in molecular systems.[1] Recently, magnetic chain compounds with large uniaxial anisotropy have been extensively investigated because many of these species were discovered to be able to exhibit not only a long-range magnetic ordering but also behaviors of single-chain magnets (SCMs).[2]

The magnetic properties of one-dimensional (1D) complexes depend on both intra- and interchain interactions. To enhance the intrachain interactions, short ligands, such as cyano,[3] hydroxyl,[4] azido,[5] oxalate/oxamate,[6] oximato,[7] and carboxylate,[8] have most commonly been employed as bridging ligands because they can efficiently transmit magnetic coupling between adjacent spin centers. The cyano group is extremely popular as an efficient and versatile mediator for magnetic coupling. A large number of cyanide-bridged complexes show a wide range of magnet types, including metamagnets,[9] room-temperature magnets,[10] spin-crossover materials,[11] single-molecule magnets (SMMs),[12] SCMs,[3,13] and photomagnets.[14]

To obtain cyanide-bridged low-dimensional bimetallic complexes, the synthetic strategies that have typically been employed previously are the following: (1) decrease the number of cyanide ligands of the hexacyanometalate $[M(CN)_6]^{3-}$ (M = Fe(III), Cr(III)), or octacyanometalate $[M(CN)_8]^{3-}$ (M = Mo(V), W(V)) precursors by blocking some of its coordination sites with chelating ligands, such as 1,10-phenanthroline, poly(pyrazolyl) borate, 2,2′-bipyridine, 2,2′-bipyrimidine, and 1,2-bis(pyridine-2-carboxamido)-benzenate;[15] (2) employ solvents, such as water, methanol, or ethanol, to adjust the structures of the final outcome;[16] (3) use metal complex fragments with coligand, such as tetradentate salen type Schiff bases (H_2SB), 2,2′-bipy, 1,10-phen, and cyclohexane-1,2-diamine instead of the hydrated mental ions.[17]

Tetradentate salen type Schiff base is a type of popular ligand which often serves as a coligand in building coordinating polymers.

Received: December 14, 2010
Published: March 28, 2011

Scheme 1. Schiff Base Ligands Used in This Study

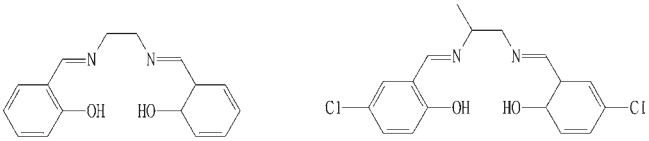

H_2salen 5-Cl-H_2salmen

Some results have been reported in which Mn^{III}−Schiff bases act as the precursors in cyanide-bridged complexes. The position and size of the substituted groups on the Schiff base ligands have been revealed to play an important role in determining the structure of resulting complexes.[18] Self-assemblies of $[Mn(SB)]^+$ and $[M(CN)_6]^{3-}$ (M = Fe(III), Cr(III), Mn(III)) or $[M(CN)_8]^{n-}$ (M = Mo(IV), Mo(V), W(IV), W(V), Nb(IV)) showed a rich variety of structures ranging from discrete compounds and 1D chains to two-dimensional (2D) networks.[16,19] There are also reports on complete coordinated three-dimensional (3D) networks based on polycyano polymetal clusters such as $[Re_6Se_8(CN)_6]^{4-}$ and $[Nb_6Cl_{12}(CN)_6]^{4-}$.[20] Some of them exhibited SMM or SCM properties induced by anisotropic sources of Mn(III).[12a,21]

In this work, we succeeded in obtaining two new cyanide-bridged magnetic chain complexes, $[\{Mn(salen)\}_2\{Mn(salen)(CH_3OH)\}\{Cr(CN)_6\}]_n \cdot 2nCH_3CN \cdot nCH_3OH$ (**1**) [$salen^{2-}$ = *N*,*N*′-ethylenebis(salicylideneiminato)-dianion] and $[Mn(5\text{-}Clsalmen)(CH_3OH)(H_2O)]_{2n}[\{Mn(5\text{-}Clsalmen)(\mu\text{-}CN)\}Cr(CN)_5]_n \cdot 5.5nH_2O$ (**2**) [5-$Clsalmen^{2-}$ = *N*,*N*′-(1-methylethylene)bis(5-chlorosalicylideneiminato) dianion], based on self-assemblies of $[Mn(salen)]^+$ or $[Mn(5\text{-}Clsalmen)]^+$ and $[Cr(CN)_6]^{3-}$, respectively. Herein, we report the syntheses, crystal structures, and magnetic properties of these two complexes.

EXPERIMENTAL SECTION

General Procedures. All the reagents were commercially available and used without further purification. The tetradentate Schiff base ligands, H_2salen and 5−Cl-H_2salmen (Scheme 1), were derived from the condensation of salicylaldehyde and 5-chloro-salicylaldehyde with 1,2-diaminoethane and 1,2-diaminopropane in a molar ratio of 2:1 in ethanol according to the literature, respectively.[22] The C, H, and N elemental analyses were carried out with a Perkin−Elmer 240C elemental analyzer. The IR spectra were recorded as KBr pellets on a Bruker Tensor 27 FTIR spectrophotometer in the 4000−400 cm^{-1} regions. Magnetic susceptibilities were measured on a Quantum Design MPMS-7 SQUID magnetometer. Diamagnetic corrections were made with Pascal's constants for all the constituent atoms.[23]

Preparation of [Mn(SB)(H$_2$O)]ClO$_4$. (SB = $salen^{2-}$ and 5-$Clsalmen^{2-}$ for complexes **1** and **2**, respectively). The manganese(III) precursors $[Mn(SB)(H_2O)]ClO_4$ were prepared by mixing $Mn(OAc)_3 \cdot 2H_2O$, H_2SB, and $NaClO_4$ in methanol-H_2O mixture with a molar ratio of 1:1:1.5, according to the method reported previously.[19b]

Preparation of [K(18-crown-6)]$_3$[Cr(CN)$_6$]. A stock solution of $[K(18\text{-crown-}6)]_3[Cr(CN)_6]$ 0.010 mmol·mL^{-1} was prepared by stirring 390.6 mg (1.2 mmol) of $K_3[Cr(CN)_6]$ and 793.8 mg (3.0 mmol) of 18-crown-6-ether in 100.0 mL of acetonitrile in the dark for 24 h. The resulting solution was filtered to remove excess $K_3[Cr(CN)_6]$.[24]

Preparation of Complex ***1***. At room temperature, the stock solution of $[K(18\text{-crown-}6)]_3[Cr(CN)_6]$ (10.0 mL) was added dropwise to a methanol solution (30.0 mL) of $[Mn(salen)(H_2O)]ClO_4$ (131.7 mg, 0.30 mmol). The mixture was stirred for 30 min and then filtered. The dark brown filtrate was left undisturbed in the dark for two weeks and brown-black single crystals of complex **1** suitable for X-ray structural analysis were obtained by slow evaporation. The crystals were collected by filtration, washed with the minimum volume of ice cold methanol-acetonitrile mixture, and dried in air. Yield: 76%. Main IR bands (KBr pellets, cm^{-1}): 3385vs, 2360w, 2122 m, 1627vs, 1600vs, 1546s, 1470s, 1445s, 1389 m, 1350s, 1334 m, 1283vs, 1209 m, 1149s, 1128 m, 1086 m, 1048 m, 977w, 905s, 859w, 800s, 765s, 631s. Elem anal. Calcd for $C_{60}H_{56}CrMn_3N_{14}O_8$ (1318.01): C, 54.68; H, 4.28; N, 14.88%. Found: C, 54.55; H, 4.30; N, 14.82%.

Preparation of Complex ***2***. Complex **2** was prepared in the same way as complex **1**, using $[Mn(5\text{-}Clsalmen)(H_2O)]ClO_4$ (156.6 mg, 0.30 mmol) instead of $[Mn(salen)(H_2O)]ClO_4$. Yield: 65%. Main IR bands (KBr pellets, cm^{-1}): 3384vs, 2129 m, 1632vs, 1531s, 1456s, 1382 m, 1318 m, 1285s, 1177 m, 1135 m, 1019 m, 934w, 875w, 809s, 721 m, 697s, 664 m. Elem anal. Calcd for $C_{29.50}H_{28.25}Cl_3Cr_{0.50}Mn_{1.50}N_6O_{7.75}$ (805.59): C, 43.98; H, 3.53; N, 10.43%. Found: C, 43.78; H, 3.66; N, 10.49%.

X-ray Crystallography. Diffraction intensities for two complexes were collected on a computer controlled Bruker SMART 1000 CCD diffractometer equipped with graphite-monochromated Mo-K_α radiation with radiation wavelength 0.71073 Å by using the ω-scan technique. Lorentz polarization and absorption corrections were applied. The structures were solved by direct methods and refined with the full-matrix least-squares technique using the SHELXS-97 and SHELXL-97 programs.[25] Anisotropic thermal parameters were assigned to all nonhydrogen atoms. The hydrogen atoms were set in calculated positions and refined as riding atoms with a common fixed isotropic thermal parameter. Analytical expressions of neutral atom scattering factors were employed, and anomalous dispersion corrections were incorporated. Crystal data and details of structural determination and refinement were summarized in Table 1.

RESULTS AND DISCUSSION

Synthesis. The assembled forms of $[Mn(SB)(H_2O)]^+$ and $[Cr(CN)_6]^{3-}$ are of great variety and dependent on Schiff base ligands, solvents, and counterions. As expected, reaction of $[Mn(SB)(H_2O)]ClO_4$ and $[K(18\text{-crown-}6)]_3[Cr(CN)_6]$ in acetonitrile-methanol mixed solvents, not in water solvent, provided the final outcome with a novel structure depending on the structure of the Schiff base. From the nonaqueous solvents, a cluster-based chain of complex **1** was synthesized, in which there is no H_2O molecule as axial ligand of Mn(III) ion. The structure of complex **1** is significantly different to the cluster $[Cr\{(\mu\text{-}CN)Mn(salen \cdot H_2O)\}_6][Cr(CN)_6] \cdot 6H_2O$,[26] in which each of the six Mn(III) ions is axially bonded to one H_2O molecule. It seems reasonable to assume that the existence of enough H_2O molecules may prevent the formation of the chain by their unique coordination-donor ability or ligand field. The advantage of $[K(18\text{-crown-}6)]_3[Cr(CN)_6]$ as Cr(III) ions resource is that it is soluble in a nonaqueous medium, such as acetonitrile and methanol solvents.

Crystal Structure of Complex 1. The crystal structure of complex **1** consists of 1D alternating neutral chains of $[\{Mn(salen)\}_2\{Mn(salen)(CH_3OH)\}\{Cr(CN)_6\}]_n$ and crystallized solvent molecules of CH_3CN and CH_3OH. A perspective view of the 1D neutral chain is shown in Figure 1, and selected bond lengths and angles are listed in Table 2.

In complex **1**, the crystallographically independent unit contains two types of $[Cr(CN)_6]^{3-}$ anions corresponding to Cr(1) and Cr(2). Both Cr(1) and Cr(2) locate on inversion centers exhibiting the usual octahedral geometry. Around the Cr(1) and Cr(2) centers, the Cr−C bonds fall in the normal range [2.064(4)−2.083(5) Å] and the C−Cr(1)−C(*cis*) and C−Cr(1 or 2)−C(*trans*) angles are all close to 90 and 180°, respectively.

dx.doi.org/10.1021/ic102495t |*Inorg. Chem.* 2011, 50, 4006–4015

Table 1. Crystallographic Data and Structural Refinement for Complexes 1 and 2

	1	2
empirical formula	$C_{60}H_{56}CrMn_3N_{14}O_8$	$C_{29.50}H_{28.25}Cl_3Cr_{0.50}Mn_{1.50}N_6O_{7.75}$
formula weight	1318.01	805.59
crystal system	triclinic	monoclinic
space group	$P\bar{1}$	$C2/c$
a (Å)	14.063(3)	37.771(8)
b (Å)	15.106(3)	11.199(2)
c (Å)	15.981(3)	19.971(4)
α (deg)	76.91(3)	90
β (deg)	80.10(3)	115.58(3)
γ (deg)	66.84(3)	90
V (Å^3)	3027.2(10)	7620(3)
Z	2	8
ρ (Mg/m^3)	1.446	1.405
absorption coefficient	0.852 mm^{-1}	0.901 mm^{-1}
F(000)	1354	3278
crystal size (mm^3)	0.20 × 0.18 × 0.08	0.20 × 0.18 × 0.06
θ range for data collection (deg)	1.81−25.02	2.39−25.02
reflections collected/unique	22372/10619 [R_{int} = 0.0461]	26724/6633 [R_{int} = 0.0588]
completeness to θ	99.5%	98.4%
max. and min transmission	0.9350 and 0.8480	0.9479 and 0.8404
data/restraints/parameters	10619/49/799	6633/63/475
goodness-of-fit on F^2	1.075	1.087
R_1 ($I > 2\sigma(I)$)	0.0622	0.0853
wR_2 ($I > 2\sigma(I)$)	0.1574	0.2137
R_1 (all data)	0.0807	0.1057
wR_2 (all data)	0.1720	0.2301

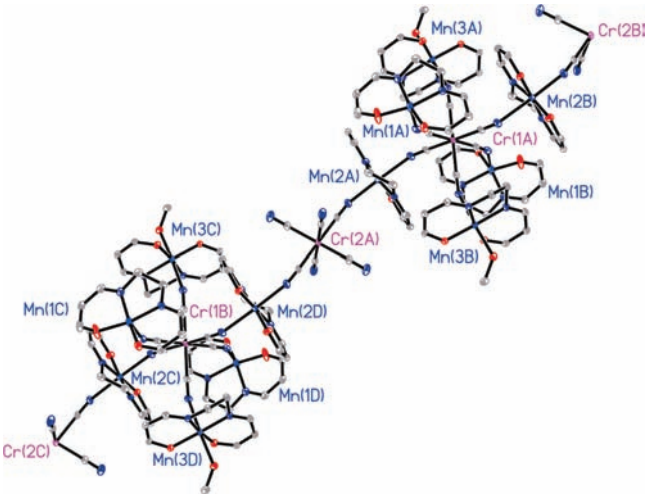

Figure 1. One-dimensional alternating chain structure of complex **1**. The hydrogen atoms and solvent molecules are omitted for clarity.

The Cr(1)−C−N angles show only slight deviation from linearity [174.6(4)−176.8(4)°], which is similar with the literature values 176.6(4)°,[26] while the Cr(2)−C−N angles show slightly less deviation from linearity [176.1(4)−179.2(4)°]. For center Cr(1), each $[Cr(CN)_6]^{3-}$ bridges four $[Mn(salen)]^+$ and two $[Mn(salen)(CH_3OH)]^+$ cations to form the $[\{Mn(salen)\}_4\{Mn(salen)(CH_3OH)\}_2\{Cr(CN)_6\}]^{3+}$ heptanuclear cation (simplified as $CrMn_6$ unit, Figure 2) with the Mn−N≡C bond angles of 143.6(3), 147.6(3) and 158.4(3)° for Mn(2)−N(2)−C(2), Mn(1)−N(1)−C(1) and Mn(3)−N(3)−C(3), respectively, which can be attributed to steric interaction between the salen^{2-} ligands on adjacent Mn(III) centers. Corresponding to center Cr(2), the $[Cr(CN)_6]^{3-}$ anion acts as a bis-monodentate ligand through two *trans*-cyano groups to bridge two $[Mn(salen)]^+$ fragments of the $CrMn_6$ units, forming an alternating neutral chain. In other words, an interesting cluster-based chainlike compound is formed by cyano-bridged clusters $CrMn_6$ extended by $[Cr(CN)_6]^{3-}$ anions. The intramolecular Mn···Cr distances through bridging cyanides are very close to each other with values of 5.169, 5.228, 5.370, and 5.331 Å for Mn(1)···Cr(1), Mn(2)···Cr(1), Mn(3)···Cr(1), and Mn(2)···Cr(2), respectively.

There are three crystallographically independent Mn(III) ions, Mn(1), Mn(2), and Mn(3), in complex **1**. Mn(1) is five-coordinated, with an equatorial plane occupied by N_2O_2 donor atoms from salen^{2-} and the axial position occupied by $N_{cyanide}$ donor atom, forming a slightly distorted square pyramid geometry. Mn(2) and Mn(3) are in a distorted octahedral geometry with the equatorial plane occupied by N_2O_2 donor atoms from salen^{2-}, and the two axial positions are occupied by $N_{cyanide}$ and $N_{cyanide}$ or $N_{cyanide}$ and $O_{methanol}$ donor atoms, respectively. Because of the Jahn−Teller distortion of the Mn(III) ions, two axial bond lengths, 2.243−2.343 (Mn−$N_{cyanide}$) and 2.272 Å (Mn−$O_{methanol}$), are relatively longer than the equatorial ones (1.874−2.001 Å), but comparable to those of $[Cr\{(\mu\text{-CN})Mn(salen\cdot H_2O)\}_6][Cr(CN)_6]\cdot 6H_2O$.[26] For Mn(2) and Mn(3), the resulting ratio of axial bond lengths to the equatorial ones are

dx.doi.org/10.1021/ic102495t |*Inorg. Chem.* 2011, 50, 4006–4015

Table 2. Selected Bond Lengths (Å) and Angles (deg) for Complex 1[a]

Cr(1)−C(2)	2.064(4)	Mn(1)−N(7)	1.973(3)
Cr(1)−C(2)#1	2.065(4)	Mn(1)−N(8)	1.979(4)
Cr(1)−C(3)	2.075(4)	Mn(1)−N(1)	2.180(4)
Cr(1)−C(3)#1	2.075(4)	Mn(2)−O(6)	1.874(3)
Cr(1)−C(1)	2.083(5)	Mn(2)−O(5)	1.888(3)
Cr(1)−C(1)#1	2.083(5)	Mn(2)−N(9)	1.991(4)
Cr(2)−C(6)#2	2.065(5)	Mn(2)−N(10)	2.001(4)
Cr(2)−C(6)	2.065(5)	Mn(2)−N(4)	2.243(4)
Cr(2)−C(4)	2.078(5)	Mn(2)−N(2)	2.343(4)
Cr(2)−C(4)#2	2.078(5)	Mn(3)−O(3)	1.879(3)
Cr(2)−C(5)	2.083(5)	Mn(3)−O(4)	1.889(3)
Cr(2)−C(5)#2	2.083(5)	Mn(3)−N(11)	1.988(3)
Mn(1)−O(2)	1.867(3)	Mn(3)−N(12)	1.994(3)
Mn(1)−O(1)	1.868(3)	Mn(3)−N(3)	2.263(4)
		Mn(3)−O(7)	2.272(3)
C(1)−N(1)−Mn(1)	147.6(3)	C(32)−N(10)−Mn(2)	125.0(3)
C(2)−N(2)−Mn(2)	143.6(3)	C(31)−N(10)−Mn(2)	113.7(3)
C(3)−N(3)−Mn(3)	158.4(3)	C(45)−N(11)−C(46)	119.8(4)
C(4)−N(4)−Mn(2)	155.7(4)	C(45)−N(11)−Mn(3)	125.7(3)
C(13)−N(7)−C(14)	119.9(4)	C(46)−N(11)−Mn(3)	114.5(3)
C(13)−N(7)−Mn(1)	126.4(3)	C(48)−N(12)−C(47)	120.5(4)
C(14)−N(7)−Mn(1)	113.2(3)	C(48)−N(12)−Mn(3)	125.3(3)
C(16)−N(8)−C(15)	120.5(4)	C(47)−N(12)−Mn(3)	113.9(3)
C(16)−N(8)−Mn(1)	126.0(3)	N(1)−C(1)−Cr(1)	175.5(4)
C(15)−N(8)−Mn(1)	113.5(3)	N(2)−C(2)−Cr(1)	174.6(4)
C(29)−N(9)−C(30)	119.1(4)	N(3)−C(3)−Cr(1)	176.8(4)
C(29)−N(9)−Mn(2)	126.5(3)	N(4)−C(4)−Cr(2)	176.1(4)
C(30)−N(9)−Mn(2)	114.3(3)	N(5)−C(5)−Cr(2)	178.8(4)
C(32)−N(10)−C(31)	121.2(4)	N(6)−C(6)−Cr(2)	179.2(4)

[a] Symmetry transformations used to generate equivalent atoms: #1 $-x$, $-y+1$, $-z+1$, #2 x, $-y+2$, $-z$.

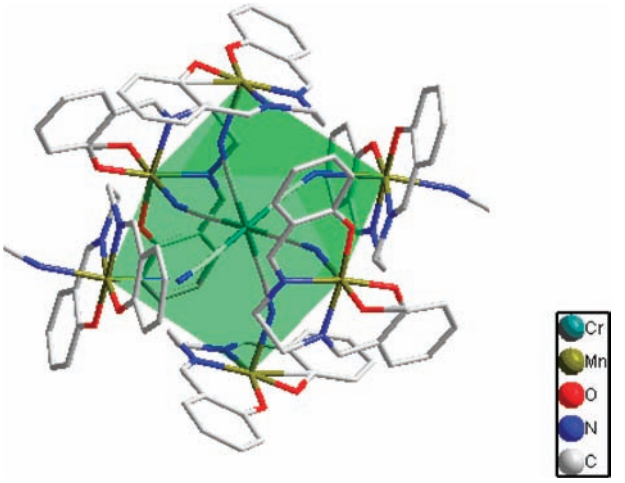

Figure 2. Coordination sphere of Cr(1) and structure of $[\{Cr(CN)_6\}\{Mn(salen)\}_4\{Mn(salen)(CH_3OH)\}_2]^{3+}$ heptanuclear ion.

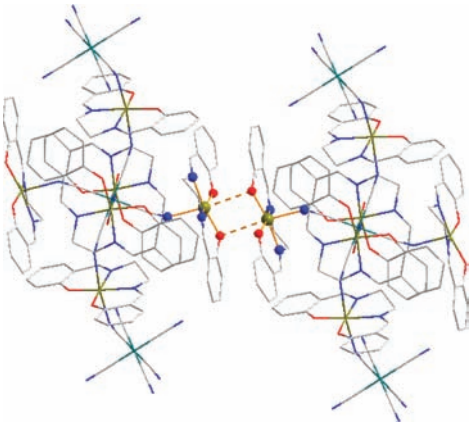

Figure 3. Structure of biphenolate bridge in complex **1**.

1.18 and 1.17, respectively, which is consistent with the corresponding ratio of 1.18 in the structure of a linear cluster $[(5\text{-Brsalen})_2(H_2O)_2Mn_2M(CN)_6]^-$ (M = Cr(III) or Fe(III)).[12a]

As shown in Figure 3, two heptanuclear cations $[\{Mn(salen)\}_4\{Mn(salen)(CH_3OH)\}_2\{Cr(CN)_6\}]^{3+}$ connect each other through the out-of-plane biphenoxo bridges -$Mn_2(O_{ph})_2$- (Mn···O^*_{ph} 3.242 Å, Mn···O−Mn* 93.2°) (O^*_{ph} is the phenolate oxygen of the neighboring molecule involved in the same out-of-plane dimer), giving rise to a unique 2D square-grid sheets (Figure 4). Therefore, the coordination polyhedron of each Mn(1) ion can also be described as an octahedron with significant axial elongation. The Mn···Mn distance in the Mn(III) dimer is 3.827 Å. The interstices between the chains and layers are occupied by solvent molecules of CH_3CN and CH_3OH. Some CH_3OH molecules form intermolecular hydrogen-bonds with the coordinated methanol oxygen atoms of $[Mn(salen)(CH_3OH)]^+$ [O(8)···O(7) = 2.611 Å] and with the terminal cyanide nitrogen atoms of $[Cr(CN)_6]^{3-}$ [O(8)···N(5) = 2.757 Å] (Supporting Information, Figure S1), respectively, which connected neighboring layers into 3D supramolecular networks. The nearest interchain Cr(III)···Cr(III) distance is 14.063 Å.

Crystal Structure of Complex 2. Complex **2** is made up of anionic straight chains $[\{Mn(5\text{-Clsalmen})(\mu\text{-CN})\}Cr(CN)_5]_n^{2n-}$, countercations $[Mn(5\text{-Clsalmen})(CH_3OH)(H_2O)]^+$, and crystallized water molecules. The structure of the straight chain and the countercation is shown in Figures 5 and 6, and selected bond lengths and angles are listed in Table 3.

For complex **2**, both Cr(1) and Mn(1) locate on inversion centers exhibiting the usual octahedral geometry. Six cyanide carbon atoms around the Cr(1) center build slightly distorted octahedral geometries with the Cr(1)−C bonds falling in the normal range [2.079(6)− 2.089(6) Å] and the C−Cr(1)−C(*cis*) and C−Cr(1)−C(*trans*) angles being all close to 90 and 180°, respectively. The Cr(1)−C≡N angles show only slight deviation from linearity [173.3(5)−178.0(5)°]. The hexacyanochromate(III) anion acts as a bis-monodentate ligand through two *trans*-cyano groups bridging two [Mn(5-Clsalmen)]$^+$ [Mn(1)] cations to form a straight chain of $[\{Mn(5\text{-Clsalmen})(\mu\text{-CN})\}Cr(CN)_5]_n^{2n-}$ with the Mn−N≡C bond angle of 151.9(4)° for Mn(1)−N(1)−C(1), having the repeating unit [−Cr−Mn−]$_n$. The Mn−N≡C entities are significantly bent, which can be attributed to the steric interaction between the 5-Clsalmen^{2-} ligands on adjacent Mn(III) centers. The intrachain Mn(1)···Cr(1) distance through bridging cyanides is 5.339 Å.

dx.doi.org/10.1021/ic102495t |*Inorg. Chem.* 2011, 50, 4006–4015

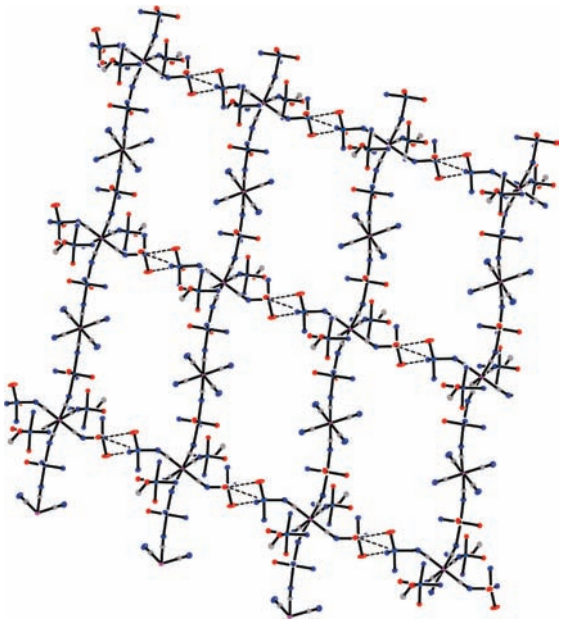

Figure 4. 2D grid-like bimetallic assemblies of complex **1.** The hydrogen atoms, solvent molecules, and carbon atoms of the Schiff base ligands are omitted for clarity.

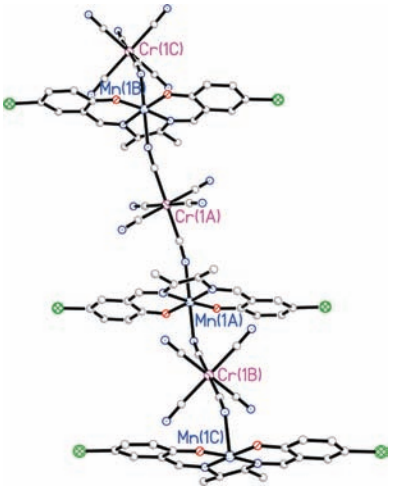

Figure 5. 1D anionic chain in complex **2**. The hydrogen atoms and solvent molecules are omitted for clarity.

The two crystallographically independent Mn(III) ions in complex **2**, Mn(1) and Mn(2), all have a distorted octahedral geometry with the equatorial plane occupied by N_2O_2 donor atoms from 5-Clsalmen^{2-}, and with the two axial positions occupied by two cyanide nitrogen atoms for Mn(1) and by two oxygen atoms from the coordinated water and methanol molecules for Mn(2). Because of the Jahn−Teller distortion of the Mn(III) ions, their axial bond lengths, 2.307(5) (Mn−$N_{cyanide}$), 2.363(6) (Mn−O_{water}), and 2.236(4) Å (Mn−$O_{methanol}$) are relatively longer than the equatorial ones (1.858−1.996 Å), but comparable to those of $[Cr\{(\mu\text{-CN})Mn(salen\cdot H_2O)\}_6][Cr(CN)_6]\cdot 6H_2O$.[26] For both Mn(1) and Mn(2), the resulting ratio of axial bond lengths to the equatorial ones is 1.19, which is consistent with the corresponding ratio in complex **1**.

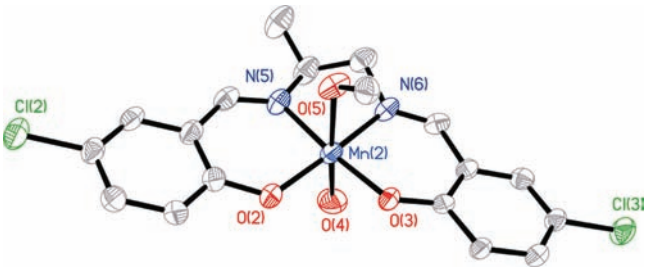

Figure 6. Perspective view of the cation $[Mn(5\text{-Cl-salmen})(CH_3OH)(H_2O)]^+$. Thermal ellipsoids set at 30% are shown.

Table 3. Selected Bond Lengths (Å) and Angles (deg) for Complex 2[a]

Mn(1)−O(1)#1	1.890(4)	Mn(2)−N(5)	1.996(5)
Mn(1)−O(1)	1.890(4)	Mn(2)−O(5)	2.236(4)
Mn(1)−N(4)#1	1.980(5)	Mn(2)−O(4)	2.363(6)
Mn(1)−N(4)	1.980(5)	Cr(1)−C(3)	2.079(6)
Mn(1)−N(1)#1	2.306(5)	Cr(1)−C(3)#2	2.079(6)
Mn(1)−N(1)	2.307(5)	Cr(1)−C(2)#2	2.080(7)
Mn(2)−O(2)	1.858(5)	Cr(1)−C(2)	2.080(7)
Mn(2)−O(3)	1.879(4)	Cr(1)−C(1)#2	2.089(6)
Mn(2)−N(6)	1.970(6)	Cr(1)−C(1)	2.089(6)
O(1)#1−Mn(1)−O(1)	93.6(2)	C(1)−N(1)−Mn(1)	151.9(4)
O(1)#1−Mn(1)−N(4)#1	92.32(17)	C(10)−N(4)−Mn(1)	125.7(4)
O(1)−Mn(1)−N(4)#1	174.04(18)	C(11)−N(4)−Mn(1)	113.4(4)
O(1)#1−Mn(1)−N(4)	174.04(18)	C(19)−N(5)−Mn(2)	124.6(5)
O(1)−Mn(1)−N(4)	92.31(17)	C(20)−N(5)−Mn(2)	113.4(4)
N(4)#1−Mn(1)−N(4)	81.8(3)	C(23)−N(6)−Mn(2)	125.3(4)
O(1)#1−Mn(1)−N(1)#1	92.68(18)	C(22)−N(6)−Mn(2)	113.2(4)
O(1)−Mn(1)−N(1)#1	91.48(18)	N(1)−C(1)−Cr(1)	173.3(5)
N(4)#1−Mn(1)−N(1)#1	89.23(19)	N(2)−C(2)−Cr(1)	178.0(5)
N(4)−Mn(1)−N(1)#1	86.17(19)	N(3)−C(3)−Cr(1)	177.3(5)
O(1)#1−Mn(1)−N(1)	91.48(18)	N(4)−Mn(1)−N(1)	89.23(19)
O(1)−Mn(1)−N(1)	92.68(18)	N(1)#1−Mn(1)−N(1)	173.9(2)
N(4)#1−Mn(1)−N(1)	86.18(19)		

[a] Symmetry transformations used to generate equivalent atoms: #1 $-x$, y, $-z+1/2$, #2 $-x$, $-y+2$, $-z$.

As shown in Figure 7, the neighboring chains of $[\{Mn(5\text{-Clsalmen})(\mu\text{-CN})\}Cr(CN)_5]_n^{2n-}$ in complex **2** are connected by the Cl···Cl weak interaction with the Cl···Cl separation of 3.461 Å to form 2D square-grid sheets. The nearest interchain Mn(III)···Mn(III) distance through Cl···Cl weak interaction is 10.564 Å. Countercations $[Mn(5\text{-Clsalmen})(CH_3OH)(H_2O)]^+$ [Mn(2)] and crystallized H_2O molecules are filled in the interspaces between chains. Thus, complex **2** is constructed by Cl···Cl weak interaction, electrostatic forces, van der Waals interactions and an extensive network of hydrogen-bonds between 1D anionic chains and countercations [N(2)···O(4) = 2.936 Å], leading to a 3D structure (Supporting Information, Figure S2).

Complexes **1** and **2** are all constructed by cyanide-bridged chains derived from manganese(III) Schiff bases and hexacyanochromate(III) building blocks. However, the two 1D chains are significantly different. In complex **1**, the ligand salen^{2-} results in the formation of heptanuclear cluster $CrMn_6$, which is

dx.doi.org/10.1021/ic102495t |*Inorg. Chem.* 2011, 50, 4006–4015

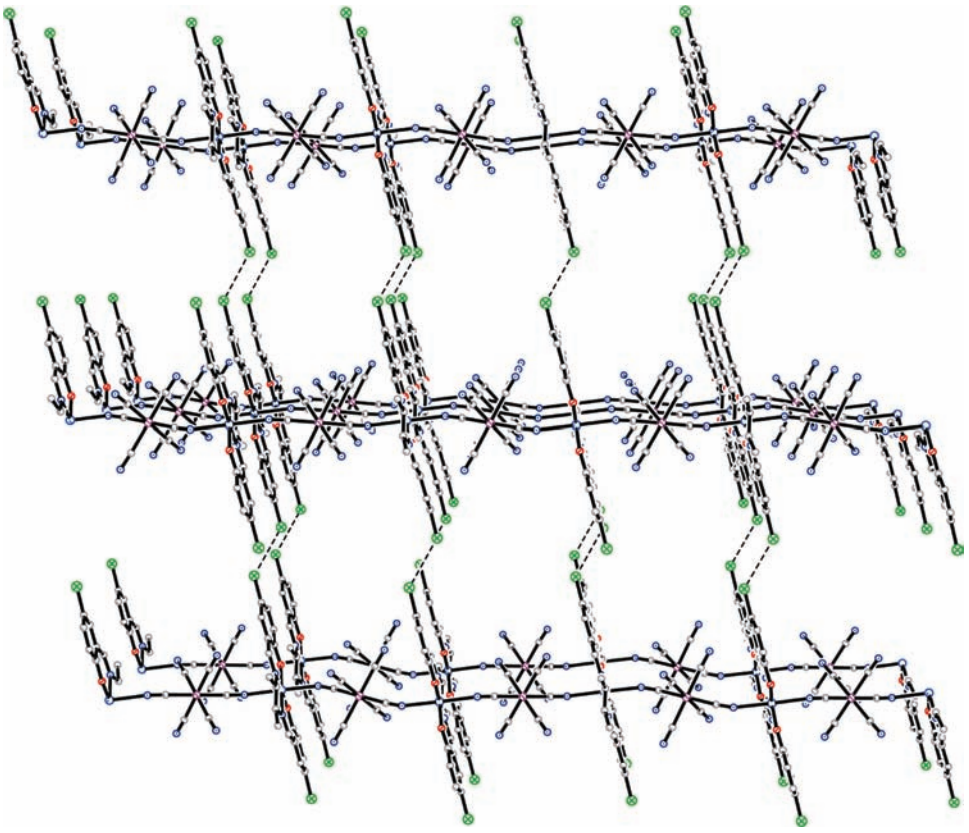

Figure 7. 2D network structure of complex **2.** The dashed line shows the Cl···Cl weak interaction.

further extended by $[Cr(CN)_6]^{3-}$ anions. While the ligand 5-Clsalmen^{2-} leads to the formation of the anionic straight chain of the repeating unit $[-Cr-Mn-]_n$ in complex **2**.

IR Spectra. The Infrared spectra of complexes **1** and **2** (Supporting Information, Figures S3 and S4) both exhibit strong broad bands centered at about 3385 cm^{-1}, which can be assigned to the ν(O−H) of the methanol (for complex **1**) or water and methanol molecules (for complex **2**). A characteristic band centered at 1628 cm^{-1} for complex **1** and 1632 cm^{-1} for complex **2** may be assigned to ν(C=N) absorption of the Schiff base group coordinated to Mn(III) ions.[26] In the 2000−2200 cm^{-1} range, a single symmetric ν_{asym}(C≡N) stretching band is observed at 2122 and 2129 cm^{-1} for complexes **1** and **2**, respectively. Just as some previously reported cyanide-bridged Cr(III)−Mn(III) analogues,[17a,26] complexes **1** and **2** contain both terminal and bridging cyanide groups, but separate cyanide absorptions are not observed in the infrared spectra. Considering the signature of the bridging cyanide is stronger than that of the terminal, we attribute the single symmetric ν_{asym}(C≡N) stretching band to the bridging cyanide groups.[3e]

Magnetic Properties of Complex 1. Magnetic measurements were carried out on crystalline samples of complexes **1** and **2** on a Quantum Design MPMS-7 SQUID Magnetometer. The temperature dependence of χ_M and $\chi_M T$ for complex **1** (χ_M being the molar magnetic susceptibility per $CrMn_3$ unit and T the temperature) in the range of 2−300 K is shown in Figure 8. The value of $\chi_M T$ at 300 K is 9.94 cm^3 K mol^{-1}, which is slightly lower than the spin-only value of 10.86 cm^3 K mol^{-1} for three uncoupled high-spin Mn(III) (S = 2) ions and one Cr(III) (S = 3/2) ion on the basis of g = 2.0. When the temperature is lowered, the $\chi_M T$ values decrease smoothly from 300 to 90 K and then sharply increase to reach a maximum value of 53.57 cm^3 K mol^{-1} at 6 K, reflecting the ferrimagnetic nature of the material. Below 6 K, the $\chi_M T$ values dropped rapidly to 11.28 cm^3 K mol^{-1} at 2 K, which may be attributed to zero-field splitting of Mn(III) ions and/or antiferromagnetic coupling between the chains.[16,18a] Considering the complicated structure of complex **1**, it is difficult to fit the magnetic data with an accurate model. Fitting the data from 300 to 90 K to the Curie−Weiss law gave C = 10.75 cm^3 K mol^{-1}, θ = −10.99 K, $R = 7.11 \times 10^{-3}$. The Curie constant is in good agreement with the expected value of 10.86 cm^3 K mol^{-1}. The negative Weiss constant indicates considerable antiferromagnetic interaction between Cr(III) and Mn(III) ions through the cyanide bridge.

At zero static field and 3.5 Oe alternating current (ac) field, the χ_M' (in-phase ac susceptibility) versus T plots at 1 and 100 Hz also display maxima at 5.0 K (Supporting Information, Figure S5). While the χ_M'' (out-of-phase ac susceptibility) values are close to zero. The maximum in $\chi'(T)$ arises as a result of long-range ordering. This clearly demonstrates that complex **1** has an antiferromagnetic ground state below a Néel temperature (T_N) of 5.0 K based on the positions of the peaks. There is no obvious frequency dependence in the $\chi_{ac}(T)$ response, which precludes any spin-glass behavior.[27] Furthermore, the zero-field cooled (ZFC) and field-cooled (FC) lines are in superposition and both show a cusp at around 5.0 K, also indicating the existence of 3D antiferromagnetic ordering for complex **1** below 5.0 K (Supporting Information, Figure S6).[18a]

The field dependence of the magnetization for complex **1** at 2 K shows a pronounced sigmoidal shape (Figure 9). The

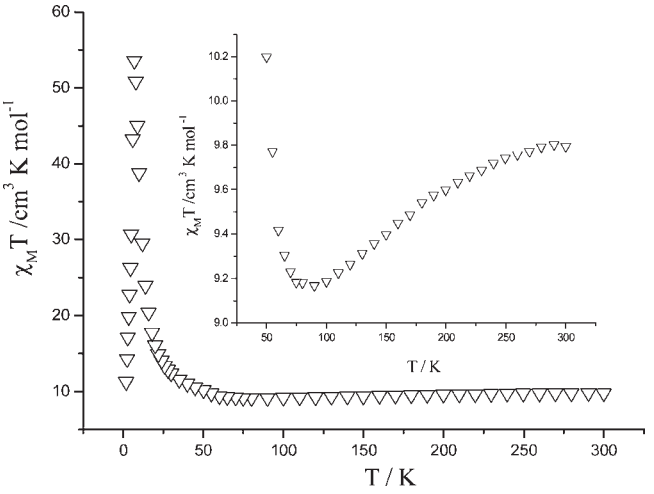

Figure 8. $\chi_M T$ versus T plot of complex **1** from 300 to 2 K. Inset: $\chi_M T$ versus T plot from 300 to 50 K of complex **1**.

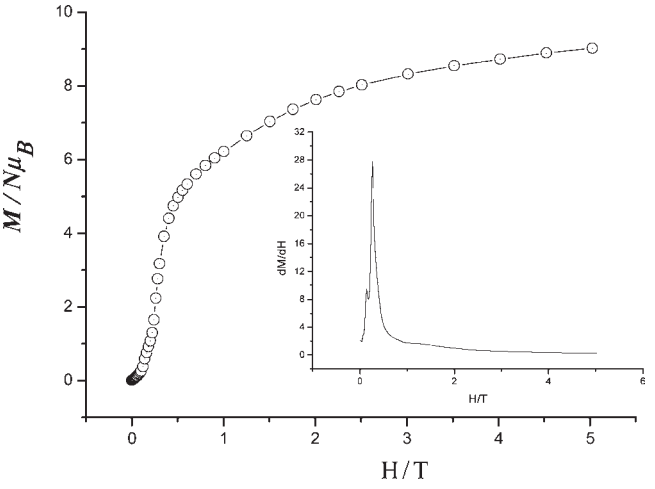

Figure 9. Magnetization as a function of the applied magnetic field for complex **1** (T = 2 K) . Inset: plot of dM/dH versus H at 2 K.

magnetization first increases very slowly with increasing field and then increases abruptly, which implies metamagnetic behavior for complex **1** that a magnetic transition occurs from the antiferromagnetic state at low field to a ferromagnetic state at high field, and the critical field defined as dM/dH at 2 K is 2.6 kOe (inset of Figure 9). The field-dependent magnetization per $CrMn_3$ unit of complex **1** at 2 K tends to a saturated value of 9.01 $N\mu_B$ at 5 T, corresponding to the expected spontaneous saturation magnetization for a ferrimagnetic ground state for $CrMn_3$ unit with S_{Mn}= 4/2 and S_{Cr}= 3/2.

To investigate the nature of the metamagnetism of complex **1**, the low temperature magnetic susceptibilities were measured at different fields (Figure 10). At applied fields lower than 5 kOe, a maximum of magnetization is observed around 4.8 K, and the maximum disappears for H > 5 kOe, suggesting a field-induced transition from an antiferromagnetic to a ferromagnetic state.[28]

As revealed by the X-ray analysis, there exist three possible exchange paths in complex **1**: (i) intrachain Mn(III)−N≡C−Cr(III) interactions via cyanide bridges, (ii) interchain Mn(III)−Mn(III) interactions via biphenolate bridges, and (iii) interlayer magnetic coupling between Cr(III) and Mn(III) through the intermolecular hydrogen-bonds.

A few cyanide-bridged Cr(III)−Mn(III) complexes usually show antiferromagnetic coupling between Cr(III) and Mn(III) ions.[12a,18a,29] The smoothly decrease of $\chi_M T$ values from 300 to 90 K supports an intrachain antiferromagnetic path in complex **1**. As the Cr(III) and Mn(III) ions possess uncompensated spins, these intrachain antiferromagnetic couplings, in fact, produce a ferrimagnetic chain. Most Mn(III)−Mn(III) dimers, in which the Mn−O*$_{Ph}$ bond distances ranges from 2.305 to 3.758 Å (O*$_{Ph}$ is the phenolate oxygen of the neighboring molecule involved in the same out-of-plane dimer), exhibit intradimer ferromagnetic exchange coupling.[16a,30] Upon increasing the Mn−O*$_{Ph}$ distance, the ferromagnetic interaction decreases, and the exchange interaction could vanish when the Mn−O*$_{Ph}$ distance reaches about 3.8 Å.[31] So we conclude that in the 2D networks of complex **1**, these chains are expected to be weakly ferromagnetically coupled through the out-of-plane double phenoxo bridges with the Mn−O*$_{Ph}$ bond distance of 3.242 Å between the two adjacent Mn(III) sites.[29a] The decrease of the $\chi_M T$ values below 5 K reflects the presence of interlayer antiferromagnetic interactions.

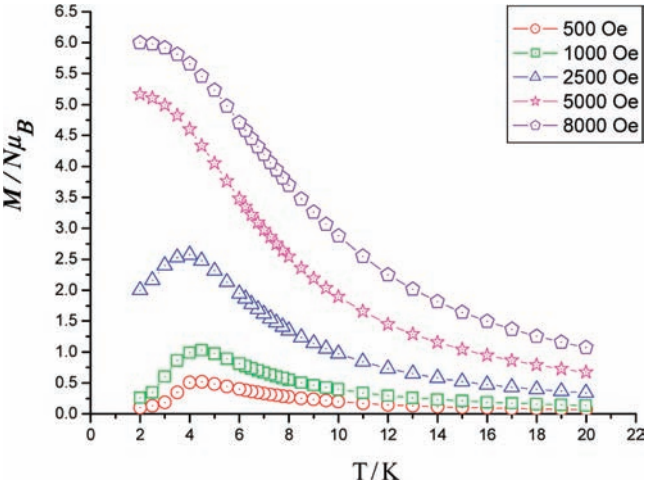

Figure 10. Magnetization as a function of the temperature for complex **1**, performed at different applied magnetic fields.

We tentatively attribute the antiferromagnetic coupling to the intermolecular hydrogen-bonds between the layers.[32] As expected, interaction through intermolecular hydrogen-bonds in complex **1** is relatively weak in comparison with the magnetic exchange through the bridging cyanide groups.

Therefore, it is easy to comprehend the metamagnetic properties according to the crystal structure of complex **1**. There exists intrachain antiferromagnetic coupling between Cr(III) and Mn(III) ions, which results in the formation of the ferrimagnetic chain and the high spin ground state of S = 9/2 per $CrMn_3$ unit. The weak antiferromagnetic interactions mediated by hydrogen-bonds lead to the antiferromagnetic ordering at 5.0 K, which could be overcome at external fields larger than 2.6 kOe, and complex **1** entered into a ferromagnetic phase.

Magnetic Properties of Complex 2. The temperature dependence of χ_M and $\chi_M T$ for complex **2** in the range of 2−300 K is shown in Figure 11 (χ_M being the molar magnetic susceptibility per $CrMn_3$ unit and T the temperature). The value of $\chi_M T$ at 300 K is 10.45 cm^3 K mol^{-1}, which is slightly lower than the spin-only value of 10.86 cm^3 K mol^{-1} for three uncoupled high-spin Mn(III)

dx.doi.org/10.1021/ic102495t |*Inorg. Chem.* 2011, 50, 4006–4015

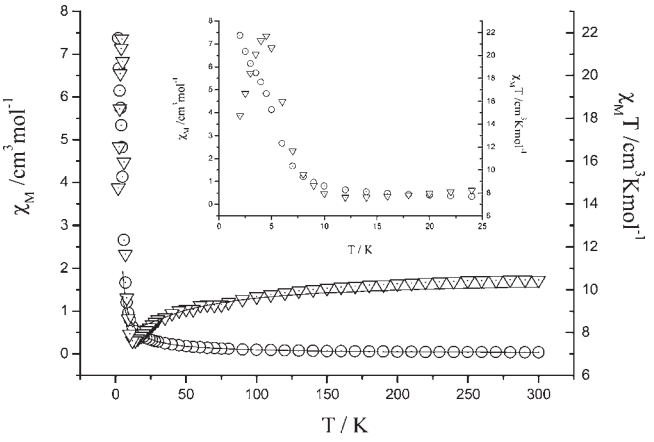

Figure 11. χ_M(O) and $\chi_M T$(Δ) versus T plots of complex **2**; the solid line is the best fitting. Inset: the expanded view of χ_M(O) and $\chi_M T$(Δ) versus T plot at low temperature (2−25 K).

($S = 2$) ions and one Cr(III) ($S = 3/2$) ion on the basis of $g = 2.0$. When the temperature is lowered, the $\chi_M T$ values decrease smoothly from room temperature until 12 K and reach a minimum value of 7.62 cm^3 K mol^{-1}, suggesting the dominant intrachain antiferromagnetic interactions as expected between Mn(III) and Cr(III) through cyanide bridges. Below 12 K, the $\chi_M T$ values sharply increase to reach a maximum value of 21.71 cm^3 K mol^{-1} at 4.5 K. These features are characteristic of ferrimagnetic chains.[33] Below 4.5 K, the $\chi_M T$ values dropped rapidly to a value of 14.74 cm^3 K mol^{-1} at 2 K, which may arise from zero-field splitting of Mn(III) ions and/or saturation effects in a 1000 G magnetic field.[34] The lack of a maximum in the χ_M versus T plot allows us to preclude the occurrence of antiferromagnetic ordering.[35]

To analyze the experimental data, Fisher's model for the classical-spin chain system ($S_A = S_{Mn} = 4/2$, $S_B = S_{Cr} = 3/2$ and $H_{chain} = -J\Sigma\hat{S}_i\hat{S}_{i+1}$) was applied to fit the magnetic susceptibility (χ_{CrMn}) of the anionic chain $[\{Mn(5\text{-Clsalmen})(\mu\text{-CN})\}Cr(CN)_5]_n^{2n-}$, which can be expressed as in eq 1:[36]

$$\chi_{CrMn} = \frac{N\beta^2}{3kT}\left[g^2\frac{1+u}{1-u} + \delta^2\frac{1-u}{1+u}\right] \quad (1)$$

$$g = (g_A^e + g_B^e)/2$$

$$\delta = (g_A^e - g_B^e)/2$$

$$u = \coth(J^e/kT) - (kT/J^e)$$

$$g_A^e = g_A[S_A(S_A+1)]^{1/2}$$

$$g_B^e = g_B[S_B(S_B+1)]^{1/2}$$

$$J^e = J[S_A(S_A+1)S_B(S_B+1)]^{1/2}$$

The contribution of the countercations $[Mn(5\text{-Clsalmen})(CH_3OH)(H_2O)]^+$ was also included as χ_{Mn} in eq 2:

$$\chi_M = \chi_{CrMn} + 2\chi_{Mn} = \chi_{CrMn} + \frac{2Ng^2\beta^2}{3kT}[S_{Mn}(S_{Mn}+1)] \quad (2)$$

where the symbols have their usual meaning, and the g factors of Mn(III) and Cr(III) are the same for simplicity. The least-squares fitting of the observed data above 8 K led to $J = -6.49$ cm^{-1} and $g = 2.05$. The agreement factor $R = \Sigma(\chi_{obsd} - \chi_{calcd})^2/\Sigma\chi^2_{obsd}$ is 7.24×10^{-3}.

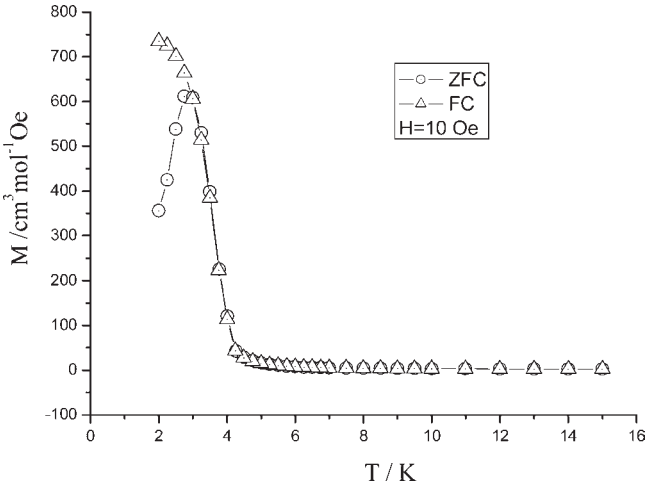

Figure 12. Zero-field-cooled magnetization(ZFCM) and field-cooled-magnetization (FCM) curve for complex **2** under a dc field of 3 Oe.

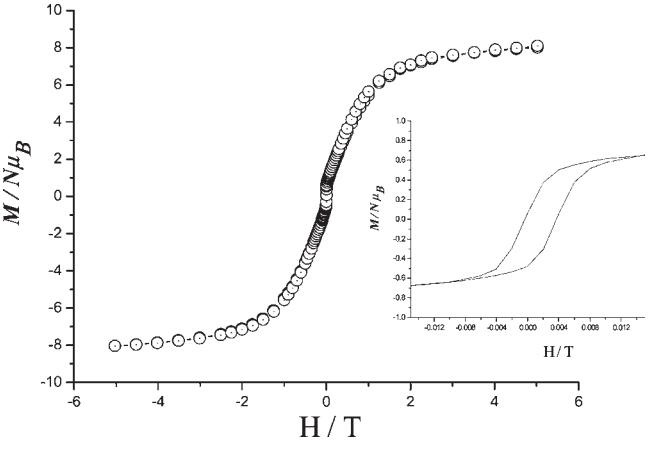

Figure 13. Hysteresis loop at 2 K for complex **2.** Inset shows the loop clearly.

As shown in Figure 12, the zero-field-cooled magnetization (ZFC) and field-cooled magnetization (FC) data at a low field of 3.0 Oe displayed irreversibility below about 3.0 K, indicating the occurrence of long-range ordering within the material, and the critical temperature, T_C, was determined as 3.0 K from the separation of ZFC and FC lines.[2c] The FC magnetization shows a plateau below this temperature typical of a complete freezing process.

Isothermal magnetization experiments performed at 2 K exhibit a hysteresis with a small coercive field of 25 Oe and a remnant magnetization of 0.28 $N\mu_B$, typical of soft magnet behavior (Figure 13). This behavior also suggests the presence of long-range ordering in complex **2** at low temperature.

CONCLUSION

This work provides two rare examples of cyanide-bridged Cr(III)−Mn(III) 1D chains based on the bridging ligand $[Cr(CN)_6]^{3-}$ and $[Mn(SB)]^+$ building blocks. The structure

dx.doi.org/10.1021/ic102495t |*Inorg. Chem.* 2011, 50, 4006–4015

and magnetic properties of the final outcome can be modulated by the steric constraints of the Schiff base ligands, solvents' coordination role, and packing effects of the counterions. Complex **1** consists of 1D alternating chains formed by the $[\{Cr(CN)_6\}\{Mn(salen)\}_4\{Mn(salen)(CH_3OH)\}_2]^{3+}$ heptanuclear cations and $[Cr(CN)_6]^{3-}$ anions. While in complex **2**, the hexacyanochromate(III) anion acts as a bis-monodentate ligand through two *trans*-cyano groups to bridge two $[Mn(5\text{-}Clsalmen)]^+$ cations to form a straight chain. The adjacent chains are then connected via the out-of-plane biphenoxo bridges (for complex **1**) or the Cl···Cl weak interaction (for complex **2**) to give the 2D layered structure. The hydrogen-bonds also play an important role in connecting the neighboring layers into 3D supramolecular networks. The magnetic analysis indicates that complex **1** shows 3D antiferromagnetic ordering with the Néel temperature of 5 K and displays antiferromagnetic to ferromagnetic transition at a critical field of about 2.6 kOe at 2 K, while complex **2** behaves as a molecular magnet with Tc = 3.0 K.

■ ASSOCIATED CONTENT

Supporting Information. CIF files of complexes **1** and **2**; a pdf file containing Figures S1−S6. This material is available free of charge via the Internet at http://pubs.acs.org.

■ AUTHOR INFORMATION

Corresponding Author

*E-mail: wangql@nankai.edu.cn (Q.-L.W.), may223@126.com (Y.M.).

■ ACKNOWLEDGMENT

This project was granted financial support from the National Natural Science Foundation of China (Nos. 21071085, 20601014, 90922032) and National Basic Research Program of China (973 Program, 2007CB815305).

■ REFERENCES

(1) (a) Kahn, O. *Molecular Magnetism*; VCH Publishers, Inc.: New York, 1993. (b) Miller, J. S.; Drillon, M. *Magnetism: Molecules to Materials*; Wiley-VCH: Weinheim, Germany, 2001−2005.

(2) (a) Visinescu, D.; Toma, L. M.; Lloret, F.; Fabelo, O.; Ruiz-Pérez, C.; Julve, M. *Dalton Trans.* **2008**, 4103. (b) Caneschi, A.; Gatteschi, D.; Lalioti, N.; Sangregorio, C.; Sessoli, R.; Venturi, G.; Vindigni, A.; Rettori, A.; Pini, M. G.; Novak, M. A. *Angew. Chem., Int. Ed.* **2001**, *40*, 1760. (c) Sun, H.-L.; Wang, Z.-M.; Gao, S. *Chem.—Eur. J.* **2009**, *15*, 1757. (d) Miyasaka, H.; Julve, M.; Yamashita, M.; Clérac, R. *Inorg. Chem.* **2009**, *48*, 3420. (e) Coulon, C.; Miyasaka, H.; Clérac, R. *Struct. Bonding (Berlin)* **2006**, *122*, 163.

(3) (a) Lescouëzec, R.; Vaissermann, J.; Ruiz-Pérez, C.; Lloret, F.; Carrasco, R.; Julve, M.; Verdaguer, M.; Dromzee, Y.; Gatteschi, D.; Wernsdorfer, W. *Angew. Chem., Int. Ed.* **2003**, *42*, 1483. (b) Wang, S.; Zuo, J. L.; Gao, S.; Song, Y.; Zhou, H. C.; Zhang, Y. Z.; You, X. Z. *J. Am. Chem. Soc.* **2004**, *126*, 8900. (c) Dunbar, K. R.; Heintz, R. A. *Prog. Inorg. Chem.* **1997**, *45*, 283. (d) Shatruk, M.; Avendano, C.; Dunbar, K. R. *Prog. Inorg. Chem.* **2009**, *56*, 155. (e) Kettle, S. F. A.; Diana, E.; Boccaleri, E.; Stanghellini, P. L. *Inorg. Chem.* **2007**, *46*, 2409.

(4) (a) Li, X. J.; Wang, X. Y.; Gao, S.; Cao, R. *Inorg. Chem.* **2006**, *45*, 1508. (b) Konar, S.; Mukherjee, P. S.; Zangrando, E.; Lloret, F.; Chaudhuri, N. R. *Angew. Chem., Int. Ed.* **2002**, *41*, 1561.

(5) (a) Xu, H.-B.; Wang, B.-W.; Pan, F.; Wang, Z.-M.; Gao, S. *Angew. Chem., Int. Ed.* **2007**, *46*, 7388. (b) Ko, H. H.; Lim, J. H.; Kim, H. C.; Hong, C. S. *Inorg. Chem.* **2006**, *45*, 8847.

(6) (a) Zhang, Y.-Z.; Wang, Z.-M.; Gao, S. *Inorg. Chem.* **2006**, *45*, 5447. (b) Pardo, E.; Ruiz-Garcia, R.; Lloret, F.; Faus, J.; Julve, M.; Journaux, Y.; Delgado, F.; Ruiz-Perez, C. *Adv. Mater.* **2004**, *16*, 1597. (c) Pardo, E.; Ruiz-Garcia, R.; Lloret, F.; Faus, J.; Julve, M.; Journaux, Y.; Novak, M. A.; Delgado, F. S.; Ruiz-Perez, C. *Chem.—Eur. J.* **2007**, *13*, 2054.

(7) (a) Miyasaka, H.; Takayama, K.; Saitoh, A.; Furukawa, S.; Yamashita, M.; Clérac, R. *Chem.—Eur. J.* **2010**, *16*, 3656. (b) Chaudhuri, P.; Weyhermüller, T.; Wagner, R.; Khanra, S.; Biswas, B.; Bothe, E.; Bill, E. *Inorg. Chem.* **2007**, *46*, 9003.

(8) (a) Zheng, Y. Z.; Tong, M. L.; Zhang, W. X.; Chen, X. M. *Angew. Chem., Int. Ed.* **2006**, *45*, 6310. (b) Bai, Y. L.; Tao, J.; Wolfgang, W.; Sato, O.; Huang, R. B.; Zheng, L. S. *J. Am. Chem. Soc.* **2006**, *128*, 16428.

(9) (a) Yoon, J. H.; Kim, H. C.; Hong, C. S. *Inorg. Chem.* **2005**, *44*, 7714. (b) Wen, H.-R.; Wang, C.-F.; Song, Y.; Gao, S.; Zuo, J.-L.; You, X.-Z. *Inorg. Chem.* **2006**, *45*, 8942. (c) Yoon, J. H.; Lim, J. H.; Choi, S. W.; Kim, H. C.; Hong, C. S. *Inorg. Chem.* **2007**, *46*, 1529. (d) Wang, S.; Ferbinteanu, M.; Yamashita, M. *Inorg. Chem.* **2007**, *46*, 610. (e) Choi, S. W.; Kwak, H. Y.; Yoon, J. H.; Kim, H. C.; Koh, E. K.; Hong, C. S. *Inorg. Chem.* **2008**, *47*, 10214. (f) Harris, T. D.; Coulon, C.; Clérac, R.; Long, J. R. *J. Am. Chem. Soc.* **2011**, *133*, 123.

(10) (a) Garde, R.; Villain, F.; Verdaguer, M. *J. Am. Chem. Soc.* **2002**, *124*, 10531. (b) Hatlevik, Ø.; Buschmann, W. E.; Zhang, J.; Manson, J. L.; Miller, J. S. *Adv. Mater.* **1999**, *11*, 914.

(11) Niel, V.; Thompson, A. L.; Muñoz, M. C.; Galet, A.; Goeta, A. E.; Real, J. A. *Angew. Chem., Int. Ed.* **2003**, *42*, 3760.

(12) (a) Choi, H. J.; Sokol, J. J.; Long, J. R. *Inorg. Chem.* **2004**, *43*, 1606. (b) Schelter, E. J.; Prosvirin, A. V.; Dunbar, K. R. *J. Am. Chem. Soc.* **2004**, *126*, 15004.

(13) (a) Ferbinteanu, M.; Miyasaka, H.; Wernsdorfer, W.; Nakata, K.; Sugiura, K.; Yamashita, M.; Coulon, C.; Clérac, R. *J. Am. Chem. Soc.* **2005**, *127*, 3090. (b) Toma, L. M.; Lescouëzec, R.; Pasán, J.; Ruiz-Pérez, C.; Vaissermann, J.; Cano, J.; Carrasco, R.; Wernsdorfer, W.; Lloret, F.; Julve, M. *J. Am. Chem. Soc.* **2006**, *128*, 4842. (c) Visinescu, D.; Madalan, A. M.; Andruh, M.; Duhayon, C.; Sutter, J.-P.; Ungur, L.; Van den Heuvel, W.; Chibotaru, L. F. *Chem.—Eur. J.* **2009**, *15*, 11808. (d) Harris, T. D.; Bennett, M. V.; Clérac, R.; Long, J. R. *J. Am. Chem. Soc.* **2010**, *132*, 3980. (e) Toma, L. M.; Lescouëzec, R.; Lloret, F.; Julve, M.; Vaissermann, J.; Verdaguer, M. *Chem. Commun.* **2003**, 1850.

(14) (a) Zhang, Y.; Li, D.; Clérac, R.; Kalisz, M.; Mathonière, C.; Holmes, S. M. *Angew. Chem., Int. Ed.* **2010**, *49*, 3752. (b) Shimamoto, N.; Ohkoshi, S.; Sato, O.; Hashimoto, K. *Inorg. Chem.* **2002**, *41*, 678.

(15) (a) Wu, D.; Zhang, Y.; Huang, W.; Sato, O. *Dalton Trans.* **2010**, *39*, 5500. (b) Choi, S. W.; Ryu, D. W.; Lee, J. W.; Yoon, J. H.; Kim, H. C.; Lee, H.; Cho, B. K.; Hong, C. S. *Inorg. Chem.* **2009**, *48*, 9066. (c) Ni, Z.-H.; Tao, J.; Wernsdorfer, W.; Cui, A.-L.; Kou, H.-Z. *Dalton Trans.* **2009**, 2788.

(16) (a) Miyasaka, H.; Matsumoto, N.; Ōkawa, H.; Re, N.; Gallo, E.; Floriani, C. *J. Am. Chem. Soc.* **1996**, *118*, 981. (b) Miyasaka, H.; Okawa, H.; Miyazaki, A.; Enoki, T. *Inorg. Chem.* **1998**, *37*, 4878.

(17) (a) Miyasaka, H.; Takahashi, H.; Madanbashi, T.; Sugiura, K.; Clérac, R.; Nojiri, H. *Inorg. Chem.* **2005**, *44*, 5969. (b) Berlinguette, C. P.; Galán-Mascarós, J. R.; Dunbar, K. R. *Inorg. Chem.* **2003**, *42*, 3416. (c) Coronado, E.; Gómez-García, C. J.; Nuez, A.; Romero, F. M.; Waerenborgh, J. C. *Chem. Mater.* **2006**, *18*, 2670.

(18) (a) Zhang, D. P.; Wang, H. L.; Chen, Y. T.; Ni, Z.-H.; Tian, L. J.; Jiang, J. Z. *Inorg. Chem.* **2009**, *48*, 11215. (b) Ni, Z.-H.; Zheng, L.; Zhang, L.-F.; Cui, A.-L.; Ni, W.-W.; Zhao, C.-C.; Kou, H.-Z. *Eur. J. Inorg. Chem.* **2007**, 1240.

(19) (a) Shen, X.; Li, B.; Zou, J.; Hu, H.; Xu, Z. *J. Mol. Struct.* **2003**, *657*, 325. (b) Przychodzeń, P.; Lewiński, K.; Balanda, M.; Pelka, R.; Rams, M.; Wasiutyński, T.; Guyard-Duhayon, C.; Sieklucka, B. *Inorg. Chem.* **2004**, *43*, 2967. (c) Yoo, H. S.; Ko, H. H.; Ryu, D. W.; Lee, J. W.; Yoon, J. H.; Lee, W. R.; Kim, H. C.; Koh, E. K.; Hong, C. S. *Inorg. Chem.* **2009**, *48*, 5617. (d) Venkatakrishnan, T. S.; Sahoo, S.; Bréfuel, N.; Duhayon, C.; Paulsen, C.; Barra, A.-L.; Ramasesha, S.; Sutter, J. -P. *J. Am. Chem. Soc.* **2010**, *132*, 6047.

(20) (a) Kim, Y.; Park, S. M.; Kim, S. J. *Inorg. Chem. Commun.* **2002**, *5*, 592. (b) Zhang, J. J.; Lachgar, A. *J. Am. Chem. Soc.* **2007**, *129*, 250.

(21) (a) Clérac, R.; Miyasaka, H.; Yamashita, M.; Coulon, C. *J. Am. Chem. Soc.* **2002**, *124*, 12837. (b) Miyasaka, H.; Clérac, R.; Wernsdorfer, W.; Lecren, L.; Bonhomme, C.; Sugiura, K.; Yamashita, M. *Angew. Chem., Int. Ed.* **2004**, *43*, 2801. (c) Miyasaka, H.; Madanbashi, T.; Sugimoto, K.; Nakazawa, Y.; Wernsdorfer, W.; Sugiura, K.-I.; Yamashita, M.; Coulon, C.; Clérac, R. *Chem.—Eur. J.* **2006**, *12*, 7028. (d) Kachi-Terajima, C.; Mori, E.; Eiba, T.; Saito, T.; Kanadani, C.; Kitazawa, T.; Miyasaka, H. *Chem. Lett.* **2010**, *39*, 94.

(22) Pfeifer, P.; Hesse, T.; Pfitzner, H.; Scholl, W.; Thielert, H. *J. Pract. Chem.* **1937**, *149*, 217.

(23) Elwood, P. W. *Magnetochemistry*; Interscience: New York, 1956; pp 78.

(24) Shatruk, M.; Dragulescu-Andrasi, A.; Chambers, K. E.; Stoian, S. A.; Bominaar, E. L.; Achim, C.; Dunbar, K. R. *J. Am. Chem. Soc.* **2007**, *129*, 6104.

(25) (a) Sheldrick, G. M. *SHELXS-97. Program for X-ray Crystal Structure Determination*; Göttingen University: Göttingen, Germany, 1997. (b) Sheldrick, G. M. *SHELXL-97. Program for X-ray Crystal Structure Determination*; Göttingen University: Göttingen, Germany, 1997.

(26) (a) Shen, X.; Li, B.; Zou, J.; Xu, Z.; Yu, Y.; Liu, S. *Trans. Met. Chem.* **2002**, *27*, 372. (b) Choi, H. J.; Sokol, J. J.; Long, J. R. *J. Phys. Chem. Solids.* **2004**, *65*, 839.

(27) Mydosh, J. A. *Spin Glasses: An Experimental Introduction*; Taylor and Francis: London, 1993.

(28) Zhang, Y.; Wang, X.-T.; Zhang, X.-M.; Liu, T.-F.; Xu, W.-G.; Gao, S. *Inorg. Chem.* **2010**, *49*, 5868.

(29) (a) Liu, X. T.; Roubeau, O.; Clérac, R. *C. R. Chim.* **2008**, *11*, 1182. (b) Miyasaka, H.; Okawa, H.; Matsumoto, N. *Mol. Cryst. Liq. Cryst.* **1999**, *335*, 303.

(30) (a) Sato, Y.; Miyasaka, H.; Matsumoto, N.; Ōkawa, H. *Inorg. Chim. Acta* **1996**, *247*, 57. (b) Shyu, H.-L.; Wei, H.-H.; Wang, Y. *Inorg. Chim. Acta* **1999**, *290*, 8.

(31) Miyasaka, H.; Clérac, R.; Ishii, T.; Chang, H.-C.; Kitagawa, S.; Yamashita, M. *J. Chem. Soc., Dalton Trans.* **2002**, 1528.

(32) Ma, Y.; Wang, K.; Gao, E.-Q.; Song, Y. *Dalton Trans.* **2010**, *39*, 7714.

(33) Miyasaka, H.; Clérac, R.; Mizushima, K.; Sugiura, K.-I.; Yamashita, M.; Wernsdorfer, W.; Coulon, C. *Inorg. Chem.* **2003**, *42*, 8203.

(34) (a) Yoo, J.; Yamaguchi, A.; Nakano, M.; Krzystek, J.; Streib, W. E.; Brunel, L.-C.; Ishimoto, H.; Christou, G.; Hendrickson, D. N. *Inorg. Chem.* **2001**, *40*, 4604. (b) Luo, Z.; Kögerler, P.; Cao, R.; Hill, C. L. *Inorg. Chem.* **2009**, *48*, 7812. (c) Papatriantafyllopoulou, C.; Stamatatos, T. C.; Wernsdorfer, W.; Teat, S. J.; Tasiopoulos, A. J.; Escuer, A.; Perlepes, S. P. *Inorg. Chem.* **2010**, *49*, 10486.

(35) Cangussu, D.; Pardo, E.; Dul, M.-C.; Lescouëzec, R.; Herson, P.; Journaux, Y.; Pedroso, E. F.; Pereira, C. L. M.; Stumpf, H. O.; Muñoz, M. C.; Ruiz-García, R.; Cano, J.; Julve, M.; Lloret, F. *Inorg. Chim. Acta* **2008**, *361*, 3394.

(36) (a) Fisher, M. E. *Am. J. Phys.* **1964**, *32*, 343. (b) Dzyaloshinsky, I. *J. Phys. Chem. Solids* **1958**, *4*, 241. (c) Moriya, T. *Phys. Rev.* **1960**, *117*, 635. (d) Wang, X.-T.; Wang, X.-H.; Wang, Z. -M.; Gao, S. *Inorg. Chem.* **2009**, *48*, 1301.